Molecular Biology of the Cell
Vol. 19, 3008–3019, July 2008

In Cultured Oligodendrocytes the A/B-type hnRNP CBF-A Accompanies MBP mRNA Bound to mRNA Trafficking Sequences

Chandrasekhar S. Raju,* Christian Göritz,* Ylva Nord,* Ola Hermanson,† Carmen López-Iglesias,‡ Neus Visa,§ Goncalo Castelo-Branco,† and Piergiorgio Percipalle*

*Department of Cell and Molecular Biology, Medical Nobel Institute, Karolinska Institute, Stockholm SE-171 77, Sweden; †Department of Neuroscience, Karolinska Institute, Stockholm SE-171 77, Sweden; ‡Serveis Cientificotècnics, Universitat de Barcelona, E-08028 Barcelona, Spain; and §Department of Molecular Biology and Functional Genomics, Stockholm University, Stockholm, SE-10691, Sweden

Submitted October 26, 2007; Revised April 8, 2008; Accepted May 6, 2008
Monitoring Editor: A. Gregory Matera

Heterogeneous ribonucleoproteins (hnRNPs) have key roles in RNA biogenesis, including pre-mRNP assembly, transport and cytoplasmic localization. Here we show by biochemical fractionation of nuclear extracts and protein–protein interaction assays that the A/B-type hnRNP CBF-A is in a multiprotein complex with hnRNP A2 and A3 and hnRNP U. Using RNA affinity chromatography and gel retardation assays, CBF-A was found to bind directly to RNA trafficking sequences in the 3′-UTR of the myelin basic protein (MBP) mRNA. In primary oligodendrocytes, astrocytes, neurons, and mouse forebrain sections, CBF-A revealed a characteristic granular cytoplasmic distribution. In mouse forebrain CBF-A–positive granules were preferentially found in regions with loosely bundled myelin fibers. In cultured oligodendrocytes, CBF-A was found to be specifically associated with endogenous MBP mRNA and CBF-A gene silencing resulted in the retention of MBP granules in the cell body. Finally, immunoelectron microscopy in differentiating oligodendrocytes showed that CBF-A is located in cytoplasmic granules that are often associated with the cytoskeleton. The results suggest that CBF-A is a novel transacting factor required for cytoplasmic mRNA transport and localization.

INTRODUCTION

Concomitantly with transcription pre-mRNA molecules become associated with heterogeneous ribonucleoproteins (hnRNPs) to form premessenger ribonucleoprotein (pre-mRNP) particles. hnRNPs comprise a large number of proteins, classified into several families based on structural and functional motifs (Dreyfuss *et al.*, 1993, 2002). In mammals, there are more than 20 major and a large number of minor hnRNP species, designated A1 to U hnRNPs (Dreyfuss *et al.*, 1993, 2002; Krecic and Swanson, 1999). Within this large protein family, hnRNPs of the A/B type exhibit a well-defined modular structure with two conserved tandemly repeated RNA-binding domains (RBDs), and a divergent C-terminal region termed auxiliary domain. Certain hnRNPs of the A/B-type are in complex with actin (Percipalle *et al.*, 2002). These proteins included the hnRNP A/B protein or CBF-A (CArG-box binding factor A; Bemark *et al.*, 1998), hnRNP A2, hnRNP A3 as well as hnRNP U (Kiledjian and Dreyfuss, 1992). Specific actin-hnRNP interactions were shown to be essential for RNA polymerase II transcription both in insect and mammalian cells, which indicates a key role for hnRNPs in mRNA synthesis (Percipalle and Visa, 2006). In addition, consistent with the idea that shuttling hnRNPs accompany mRNA transcripts from gene to polysomes, a number of other specialized functions have been ascribed to the A/B-type hnRNPs, including a role in mRNP export, cytoplasmic transport, and localization (Dreyfuss *et al.*, 2002).

In the cytoplasm, mRNA transport and localization have been studied in *Drosophila melanogaster*, *Xenopus laevis* oocytes, yeast and, more recently, in mammalian somatic cells (Palacios and St. Johnson, 2001; Shav-Tal and Singer, 2005). *cis*-acting sequences in the RNA and cellular transacting factors mediate cytoplasmic transport and localization of many eukaryotic mRNAs, including β-actin mRNA in fibroblasts (Ross *et al.*, 1997; Hüttelmaier *et al.*, 2005), Vg1 mRNA in *X. laevis* oocytes (Deshler *et al.*, 1997) and myelin basic protein (MBP) mRNA in oligodendrocytes (Ainger *et al.*, 1993, 1997). For transport of MBP mRNP granules to the myelin compartment, a 21-nucleotide sequence in the 3′-untranslated region (UTR), known as RTS (RNA trafficking sequence), works as *cis*-acting sequence and is necessary and sufficient for MBP mRNA transport (Ainger *et al.*, 1997). In vitro, the RTS is recognized by the transacting factors hnRNP A2 and A3, which are presumably part of transported granules. In oligodendrocytes, hnRNP A2 was found to facilitate transport of microinjected RTS-containing transcripts and a similar role in RTS-mediated mRNA trafficking was suggested for hnRNP A3 in hippocampal neurons (Hoeck *et al.*, 1998; Carson *et al.*, 2001; Ma *et al.*, 2002; Smith, 2004; Carson and Barbarese, 2005).

This article was published online ahead of print in *MBC in Press* (http://www.molbiolcell.org/cgi/doi/10.1091/mbc.E07–10–1083) on May 14, 2008.

Address correspondence to: Piergiorgio Percipalle (piergiorgio.percipalle@ ki.se).

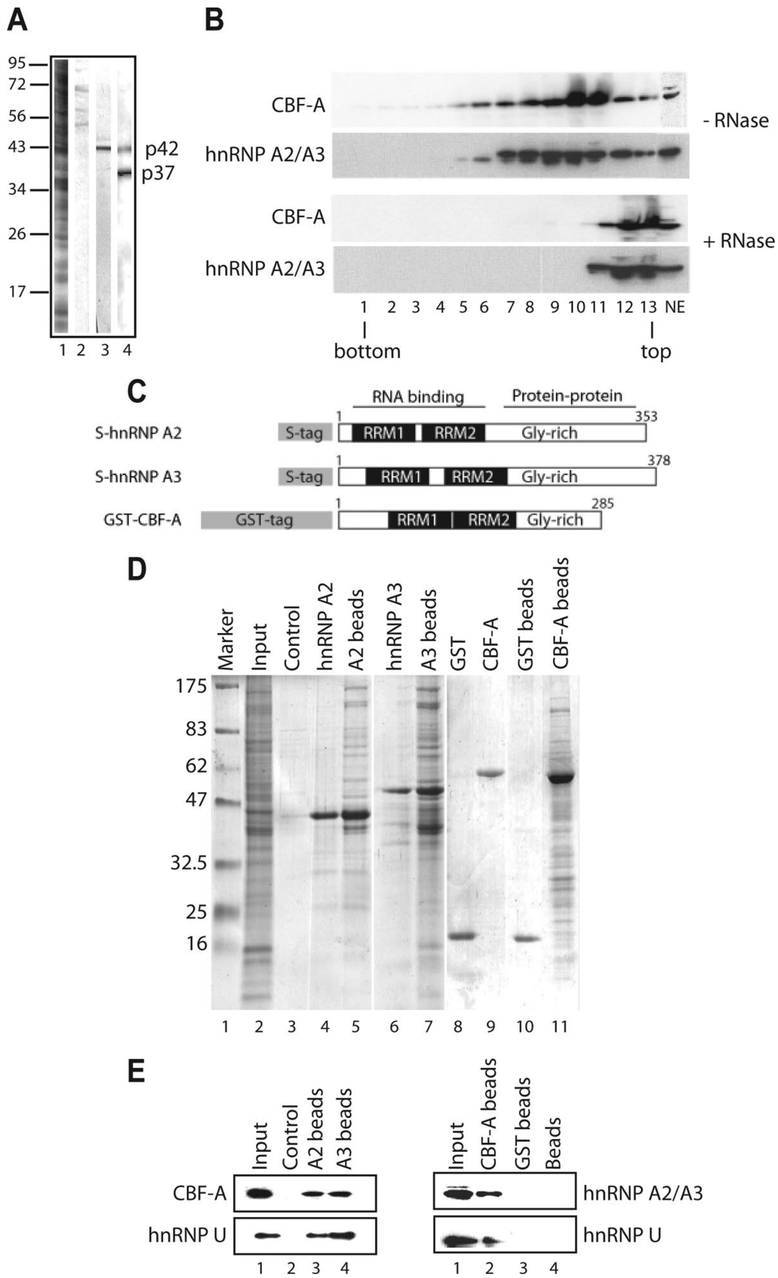

Figure 1. CBF-A, hnRNP A2, hnRNP A3, and hnRNP U are part of the same multiprotein complex. (A) Specificity of the affinity-purified peptide specific polyclonal anti-CBF-A antibody. Total protein extracts from HeLa cells were resolved by SDS-PAGE, blotted, and stained with Coomassie Blue (lane 1), immunostained with the CBF-A preimmune serum (lane 2), or with the affinity-purified anti-CBF-A antibody (lane 3) and with antibody SAK22 recognizing both CBF-A isoforms p37 and p42 (lane 4). (B) Sucrose gradient analysis of CBF-A, hnRNP A2, and hnRNP A3 from HeLa nuclear extracts. Fractions were resolved by SDS/PAGE and analyzed on immunoblots with antibodies to CBF-A and hnRNP A2/A3. (C) Schematic representation of recombinant hnRNP A2 and A3 and CBF-A constructs. (D) Pulldown experiment using S-tagged hnRNP A2, S-tagged hnRNP A3, or GST-tagged CBF-A constructs. The beads were incubated with HeLa nuclear extracts. Bound proteins were resolved by SDS PAGE, revealed by Coomassie staining and (E) analyzed on immunoblots with antibodies to CBF-A, hnRNP A2 and A3, and hnRNP U.

MBP, together with the proteolipid protein (PLP) and its isoform DM20 are major constituents of purified myelin, and they are required to stabilize the apposed myelin membranes in compact myelin (Gielen *et al.*, 2004). The molecular mechanisms underlying the regulation of MBP biogenesis are still unclear. In an attempt to identify transacting factors associated with transported granules, recent proteomic studies showed that hnRNP U and CBF-A are among the hnRNPs that are found in RNP granules isolated from developing and adult mouse brains (Kanai *et al.*, 2004; Elvira *et al.*, 2006). CBF-A is a shuttling hnRNP component of pre-mRNP/mRNP particles (Percipalle *et al.*, 2002). However, despite of the above observations, at this stage, its potential role in cytoplasmic mRNA transport and MBP biogenesis has not yet been investigated.

In this study, we show evidence that CBF-A binds the MBP mRNA RTS sequence and is required in vivo for MBP mRNA transport in oligodendrocytes. Based on these observations, we propose a general role for CBF-A as a cellular transacting factor in cytoplasmic RNA transport and localization.

MATERIALS AND METHODS

Antibodies

The rabbit polyclonal peptide specific antibody to CBF-A was raised using the peptide YQQGYGPGYGGYDY as antigen. The same peptide antigen conjugated to Sulfolink resin (Pierce, Rockford, IL) was used for affinity purification of the serum. The rabbit polyclonal antibody (SAK22) against p37 and p42 CBF-A isoforms was a gift from J. Dean (Imperial College of Science, London; see also Supplementary Information).

Cell Culture

HeLa and oli-neu cells (gift from J. Trotter, University of Mainz) were maintained as previously shown (Jung *et al.*, 1995; Percipalle *et al.*, 2002). Briefly,

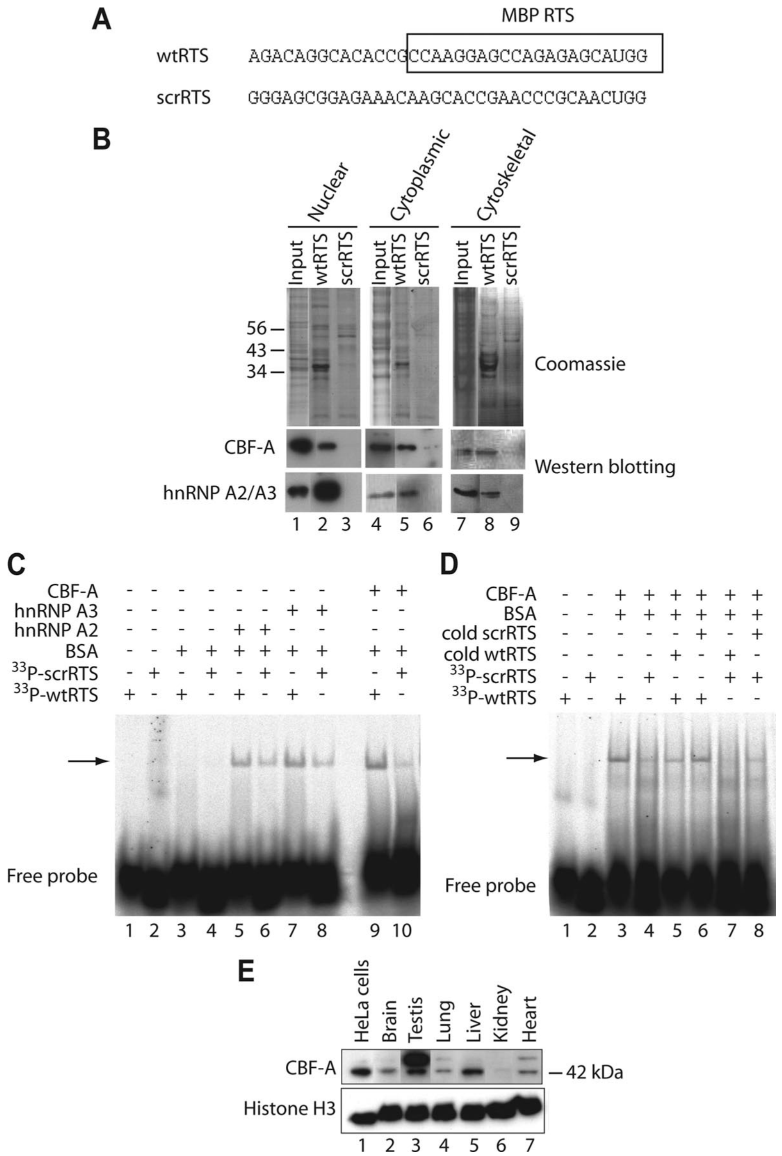

Figure 2. CBF-A binds the MBP mRNA RTS. (A) Sequences of wild-type (wtRTS) and scrambled RTS (scrRTS) used in this study. (B) Biotinylated wtRTS and scrRTS were conjugated to streptavidin Sepharose. Beads were incubated with HeLa nuclear, cytoplasmic, and high-salt protein extracts. Bound proteins were resolved by SDS-PAGE, revealed with Coomassie, and analyzed on immunoblots with antibodies to CBF-A and hnRNP A2 and A3. (C) RTS-binding assays using ^{33}P-labeled wtRTS and scrRTS sequences. To perform EMSA, wtRTS and scrRTS probes were incubated with purified CBF-A and hnRNP A2 and A3 without affinity tags or (D) in the presence (+) or absence (−) of a 25-fold excess of unlabeled competitor RNA oligonucleotides as indicated. (E) Tissue distribution of CBF-A, analyzed on immunoblots, and normalized to the steady-state expression of histone H3.

oli-neu cells were propagated in Sato medium containing 1% horse serum and differentiated for 7–10 d with dibutyryl cAMP (Sigma-Aldrich, St. Louis, MO), as described (Jung *et al.,* 1995).

Immunohistochemistry on Mouse Forebrain Sections

Adult C57bl6 mice (Charles River, Wilmington, MA) were transcardially perfused with PBS followed by 4% formaldehyde in PBS, and brains were dissected and postfixed overnight at 4°C. Coronal sections were made at 35 μm using a vibratom (Leica, Heidelberg, Germany). Immunostaining for CBF-A, MBP, and CNPase was performed on free-floating sections (see Supplementary Information).

Primary Cells

Adult mouse neural stem cells were prepared and cultured as neurospheres and differentiated as described (Rietze and Reynolds, 2006), with minor modifications (see Supplementary Information for a detailed description of the protocol used). Fetal rat neural stem cells were prepared as described in the Supplementary Information.

Immunofluorescence Microscopy, Immuno-FISH, and Gene Silencing

Immunofluorescence and immuno-FISH on cells grown on coverslips were already described (Singer and Ward, 1982; Percipalle *et al.,* 2002). For in situ detection of MBP mRNA, the RNA probe 5′-CCAUGCUCUCUGGCUCCU-UGGCGGUGUGCCUGUCU-3′ was digoxigenin-labeled in the 5′ end. Confocal images were collected using a Zeiss LSM 510 META confocal laser scanning microscope (Jena, Germany; Percipalle *et al.,* 2002).

For posttranscriptional silencing of the *CBF-A* gene, the siGENOME SMART pool duplex against the mouse *HNRPAB* gene (NM_010448) or the control ECFP (enhanced cyan fluorescent protein) gene were transfected into oli-neu cells according to the manufacturer's instructions (Dharmacon Research, Boulder, CO). Sequences can be found in Supplementary Information.

Cloning, Expression, and Protein Purification

Full-length hnRNP A2 (forward primer 5′-GGAATTCTTAGCGACTGAGTC-CGCGATG, reverse primer 5′-ATAAGAATGCGGCCGCTGAAGCTGTTCT-GTTACCTCTG) and hnRNP A3 (Ma *et al.,* 2002) were cloned in pGEM-T (Promega, Madison, WI) and subsequently in pET30a (+) for expression (Novagen, Madison, WI). Constructs were verified by DNA sequencing. Full-length glutathione *S*-transferase (GST)-tagged CBF-A (gift of Tomas Leanderson, Lund University) was expressed from a pGEX plasmid vector (see Supplementary Information).

Protein–Protein Interaction Assays

For pulldown experiments, recombinant hnRNP A2, hnRNP A3, or CBF-A constructs were coupled to protein S agarose or glutathione beads (Novagen; GE Healthcare, Waukesha, WI) and incubated with HeLa nuclear extracts (see Supplementary Information).

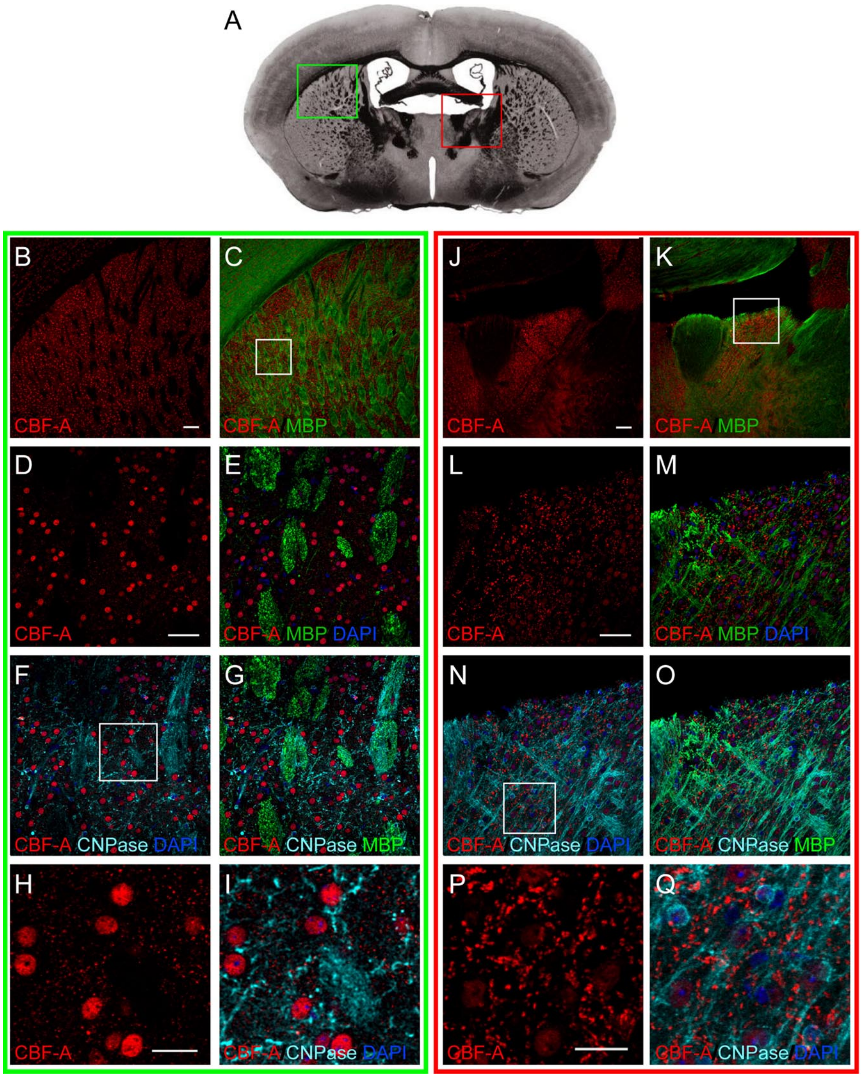

Figure 3. In vivo distribution of CBF-A in the adult mouse forebrain. (A) Coronal section of the septo-diencephalic region, showing the myelin distribution. Rectangles indicate the analyzed regions: green rectangle shown in the left panel (B–I); red rectangle shown in the right panel (J–Q). Panel A was adapted from the High Resolution Mouse Brain Atlas (Sidman *et al.*, 2008; http://www.hms.harvard.edu/research/brain/atlas.html.) (B–Q) Distributions of CBF-A, MBP, and CNPase. (B–I) The striatum with characteristic myelin bundles stained for MBP in green. In this region CBF-A can be detected in nuclei and small granular structures. CBF-A granular structures appear in close proximity to CNPase-positive membranes and MBP. (J–K) The region around the third ventricle and (L–Q) specifically the anterior thalamic nucleus. In this region CBF-A is found in larger clusters (granules) along myelin fibers. Scale bars, (B and J) 100 μm; (D and L) 50 μm; (H and P) 20 μm.

Protein and RNA Immunoprecipitation

For protein immunoprecipitations, total protein extracts prepared from oli-neu cells were incubated with the anti-CBF-A antibody, with the anti-HA tag antibody, and with nonspecific mouse IgGs. Where indicated, extracts were incubated with RNase A (see Supplementary Information). The immunoprecipitated fractions from untreated and RNase A–treated extracts were resolved by SDS-PAGE and analyzed on immunoblots with antibodies against CBF-A and hnRNP A2. For analysis of the RNA species associated with CBF-A, the RNA was extracted from the fractions immunoprecipitated with the anti-CBF-A antibody or mock and IgG control immunoprecipitation assays using the Trizol reagent, followed by DNase I (Invitrogen, Carlsbad, CA) treatment and subsequently made into cDNA by Superscript II (Invitrogen) using random primers. The samples were then analyzed by quantitative RT-PCR (qRT-PCR) with primers specific to MBP mRNA exon 1, MBP mRNA exon 2, and Sox 10 and Sox9 mRNA (see Supplementary Information for primer sequences and qRT PCR analysis).

Protein–RNA Interaction Assays

RNA affinity chromatography was performed as described (Hoek *et al.*, 1998). For each RNA-binding experiment, 500 pmol of 5′-biotinylated wild-type RTS (wtRTS; 5′-AGACAGGCACACCGCCAAGGAGCCAGAGAGCAUGG-3′) and scrambled RTS (scrRTS; 5′-GGGAGCGGAGAAACAAGCACCGAAC-CCGCAACUGG-3′) were coupled to streptavidin-coated Sepharose (GE Healthcare) and incubated with nuclear, cytoplasmic, and high-salt extracts. Bound proteins were resolved by SDS-PAGE and analyzed on immunoblots (see Supplementary Information).

For electrophoretic mobility shift assay (EMSA), wtRTS, and scrRTS were 5′ end-labeled using γ-^{33}P-ATP (GE Healthcare) and T4 polynucleotide kinase (New England Biolabs, Beverly, MA). Purified hnRNP A2, hnRNP A3, and CBF-A were incubated with ~50 fmol of ^{33}P-labeled wtRTS or scrRTS in EMSA buffer (20 mM HEPES, pH 7.6, 5 mM $MgCl_2$, 40 mM KCl, 1 mM DTT, 5% glycerol) containing heparin (5 μg/μl) and BSA (100 μg/ml) for 30 min on ice. Protein–RNA complexes were resolved by native gel electrophoresis and analyzed with a Fuji-BAS 2000 phosphorimager (Tokyo, Japan).

Immunoelectron Microscopy

After fixation, the cells were either cryosectioned or cryosubstituted and embedded in Lowicryl K4M (Polysciences, Warrington, PA; see Supplementary Information). Cryosectioned samples provided a good definition of nuclear and membrane structures, whereas cryosubstitution offered a superior preservation of the cytoskeleton. For immunolabeling, binding of the anti-CBF-A antibody was detected with either a secondary antibody or protein A coupled to 10-nm diameter colloidal gold particles. Sections were observed in a JEM-1010 electron microscope (Jeol, Tokyo, Japan), and photographic negatives were scanned with an Artixcan 2500f scanner (Microtek International, Hsinchu, Taiwan; see Supplementary Online Information).

RESULTS

CBF-A, hnRNP A2 and A3, and hnRNP U Are Present in a Multiprotein Complex

CBF-A is present in two alternatively spliced isoforms, p37 and p42, that differ only for the presence of a 47-amino acid insert in the p42 C-terminus located outside their RNA-binding domains (Dean *et al.*, 2002). Evidence that CBF-A is

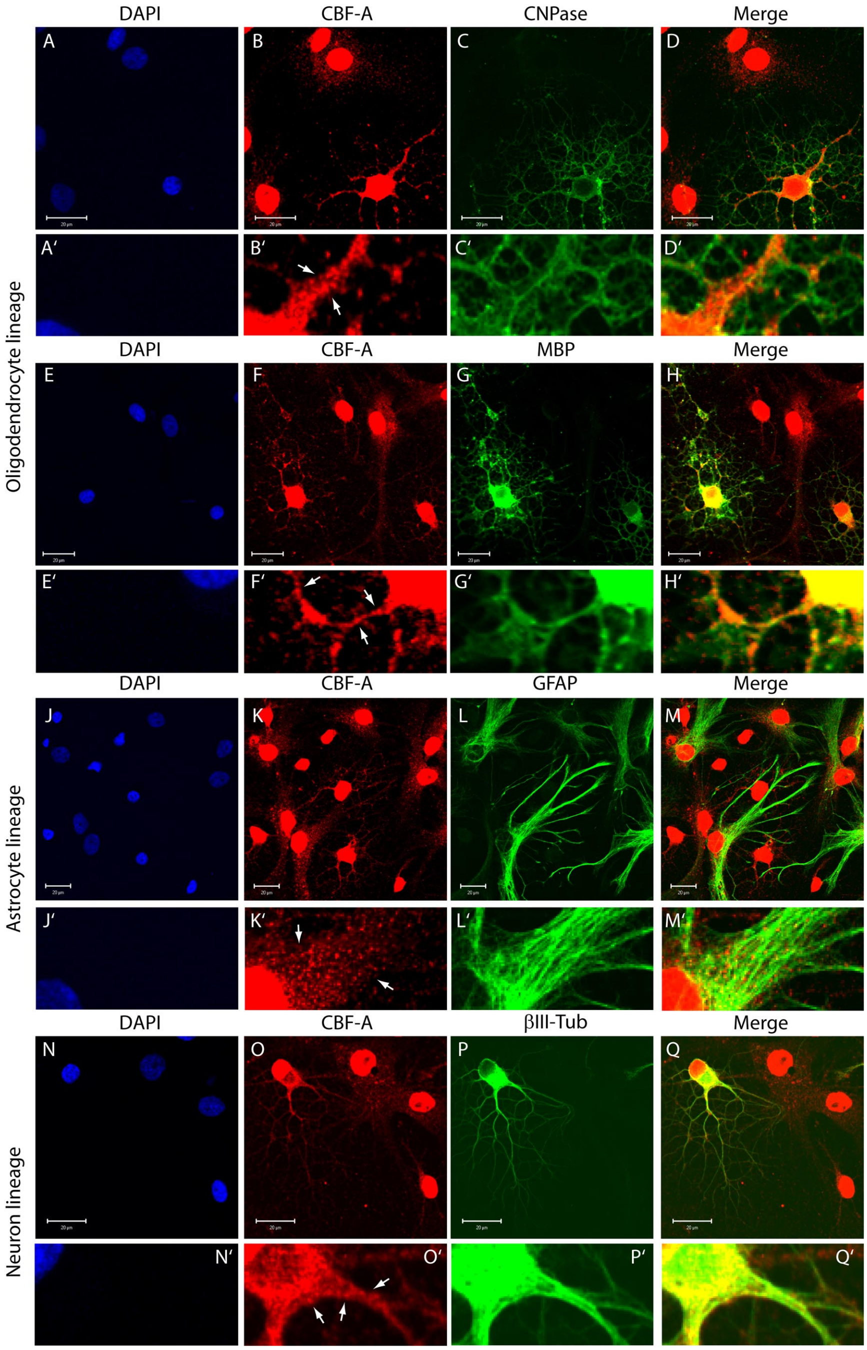

Figure 4. In primary cells CBF-A is present in cytoplasmic granules. Fetal rat neural stem cells were differentiated to oligodendrocyte, astrocyte, and neuron lineages and stained with the anti-CBF-A antibody and an anti-CNPase (A–D and magnifications A′–D′) or anti-MBP mAb (E–H and magnifications E′–H′), with anti-CBF-A and anti-GFAP antibody (J–M and magnifications J′–M′) and with anti-CBF-A and a monoclonal anti-βIII-tubulin antibody, respectively. In all cases arrows identify examples of CBF-A granular staining. Scale bar, 20 μm.

a component of pre-mRNP/RNP particles prompted us to determine whether CBF-A is in a multiprotein complex together with core hnRNP proteins such as hnRNP A2 and hnRNP A3. We first fractionated nuclear proteins prepared from HeLa cells by ultracentrifugation on a sucrose gradient and monitored coelution of CBF-A on immunoblots, using a novel affinity-purified peptide-specific anti-CBF-A antibody that recognizes the larger p42 isoform (Figure 1A, cf. lane 3). CBF-A was found to coelute with hnRNP A2/A3 in an RNA-dependent manner (Figure 1B). To demonstrate the suggested association of CBF-A with hnRNP A2/A3, tagged CBF-A, hnRNP A2, and hnRNP A3 full-length constructs were recombinantly expressed and affinity-purified for in vitro protein–protein interactions (Figure 1C). GST-tagged CBF-A and S-tagged hnRNP A2 and A3 were coupled to either glutathione beads or protein S beads and incubated with HeLa nuclear protein extracts. Coprecipitated proteins were resolved by SDS-PAGE and monitored on immunoblots. Figure 1E shows that recombinant CBF-A, hnRNP A2, and hnRNP A3 reciprocally coprecipitated the endogenous proteins, as well as hnRNP U, a newly identified protein component of transported RNA granules (Elvira *et al.*, 2006; Kanai *et al.*, 2004). None of the proteins could be coprecipitated from nuclear extracts using protein S beads or GST beads, further supporting the specificity of the reaction (Figure 1D, cf. lanes 3and 10, and Figure 1E). Overall, these results are consistent with the view that subcellular fractions of CBF-A, hnRNP A2, hnRNP A3, and hnRNP U are phys-

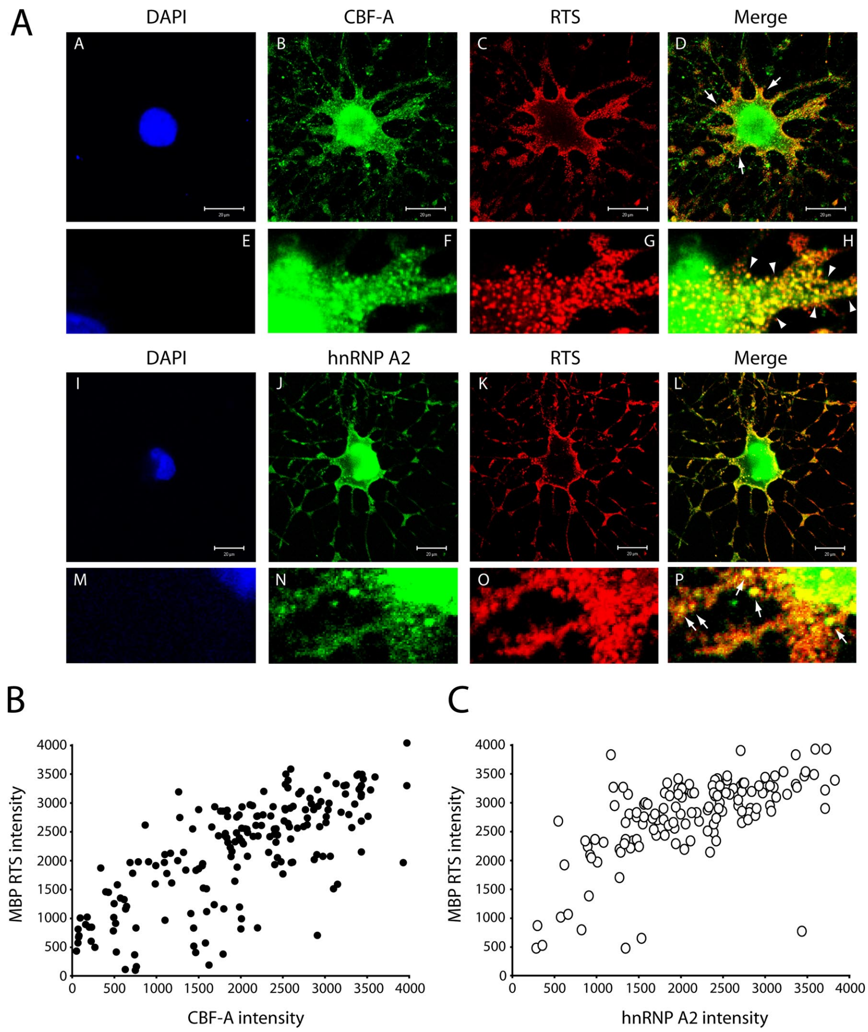

Figure 5. In cultured oligodendrocytes, CBF-A exhibits a granular cytoplasmic distribution which correlates with transported MBP mRNA. (A) Endogenous CBF-A (A–D and E–H) or (hnRNP A2 I–L and M–P) and MBP mRNA were simultaneously monitored by immuno-FISH and confocal microscopy. In D, arrows identify sites in which the distribution of CBF-A correlates with MBP RTS along processes. In E–H and M–P, oligodendrocyte processes are shown at approximately fivefold higher magnification. In H, arrowheads identify examples of CBF-A and MBP RTS-positive granules. In P, arrows point to examples of hnRNP A2- and MBP mRNA-positive granules. Scale bar, 20 μm. (B) Unbiased statistical quantification of individual CBF-A and MBP RTS-positive granules and (C) hnRNP A2 and MBP RTS-positive granules based on the immuno-FISH analysis. In both cases a linear correlation between the fluorescence intensity levels of CBF-A and RTS or hnRNP A2 and RTS is revealed.

ically associated and are contained in a nuclear multiprotein complex.

CBF-A Binds the MBP RTS

The finding that CBF-A is in a complex with hnRNP A2, hnRNP A3, and hnRNP U suggests that CBF-A may also be associated with MBP mRNA either indirectly or directly bound to the RTS sequence. To analyze this possibility, we synthesized biotinylated 35-nt RNA oligonucleotides encompassing the wtRTS from MBP mRNA and scrRTS with identical nucleotide composition but a different primary sequence (Figure 2A). To test whether endogenous CBF-A associated with RTS sequences, we coupled wtRTS and scrRTS to streptavidin-coated Sepharose beads and incubated the beads with HeLa nuclear, cytoplasmic, or high-salt (or cytoskeletal) protein extracts. The blots in Figure 2B show that endogenous CBF-A and hnRNP A2 and A3 coprecipitated with wtRTS from all cellular extracts (cf. lanes 2, 5, and 8), whereas no significant levels of CBF-A and hnRNP A2 and A3 were coprecipitated with scrRTS beads (Figure 2B, cf. lanes 3, 6, and 9).

We next applied EMSAs to determine whether CBF-A directly binds the RTS motif. We incubated ^{33}P-labeled wtRTS and scrRTS RNA oligonucleotides with purified CBF-A (37-kDa isoform), hnRNP A2, or hnRNP A3, where the affinity tags had been proteolytically removed. Figure 2C shows that the electrophoretic mobility of the wtRTS oligonucleotide was considerably retarded when incubated with CBF-A, whereas the electrophoretic mobility of scrRTS was only marginally affected by CBF-A (Figure 2C, cf. lanes 9 and 10). Similar results were obtained with hnRNP A2 and A3 used as control (Figure 2C). In comparison with wtRTS, the electrophoretic mobility of scrRTS was only slightly retarded when incubated with CBF-A (Figure 2D, cf. lanes 3 and 4). Second, retardation in the electrophoretic mobility of wtRTS incubated with CBF-A was altered in the presence of unlabeled wtRTS but not in the presence of unlabeled scrRTS when added in large excess to the reaction mixture (Figure 2D, cf. lanes 3, 5 and 3, 6, respectively). Finally, incubation of CBF-A with labeled scrRTS was sensitive to competition with unlabeled wtRTS but was not sensitive to competition with unlabeled scrRTS (Figure 2D, cf. lanes 4, 7 and 4, 8). These results indicate that CBF-A specifically binds the MBP mRNA RTS, presumably as part of a multiprotein complex.

In Oligodendrocytes CBF-A Associates with MBP mRNA Granules

If CBF-A specifically binds RTS sequences found within the MBP mRNA, it is possible that in oligodendrocytes CBF-A remains associated with transported mRNA granules outside the cell nucleus. Consistently, immunoblots of protein

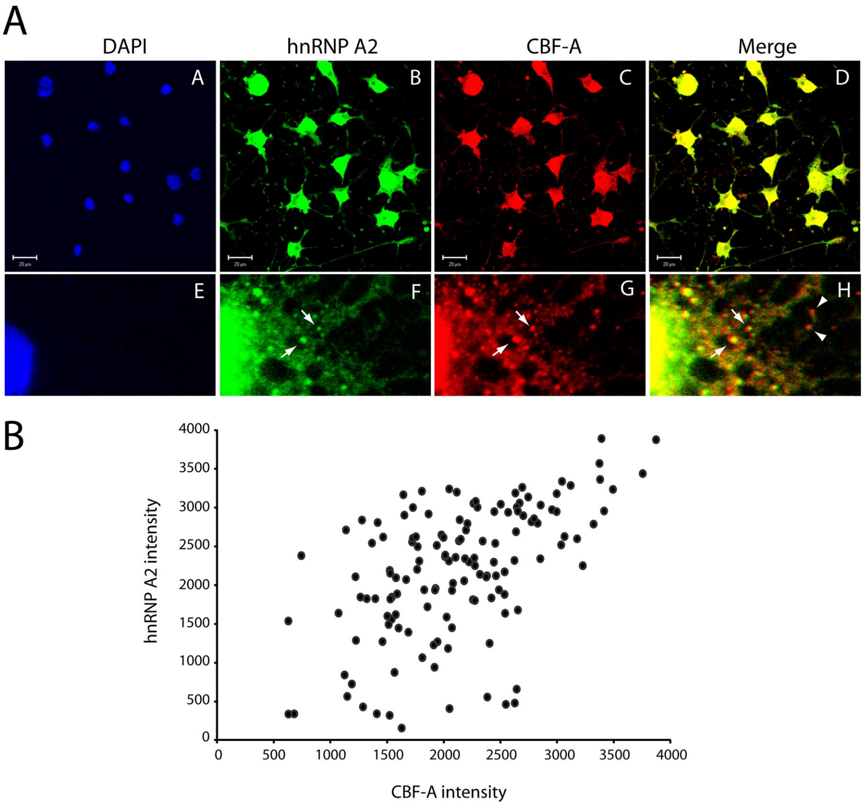

Figure 6. In oli-neu cells, the distribution of endogenous CBF-A correlates with hnRNP A2. (A and E) DAPI staining, (B and F) oli-neu cells stained with a mAb to hnRNP A2. (C and G) Oli-neu cells stained with the rabbit polyclonal peptide-specific anti-CBF-A antibody and (D and H) merged images. Scale bar, 20 μm. (B) Statistical quantification of CBF-A and hnRNP A2-positive granules based on the double immunofluorescence analysis and confocal microscopy in A. A linear correlation between the fluorescence signals of CBF-A and hnRNP A2 is revealed.

extracts prepared from different mouse tissues revealed that CBF-A is ubiquitously expressed (Figure 2E) and that the anti-CBF-A antibody is monospecific in brain tissue (Figure 2E, lane 2).

On the basis of the above, we analyzed the in vivo distribution of CBF-A in the myelin-rich regions present in the forebrain of adult mice. In agreement with its ubiquitous expression, immunostaining of mouse brain sections with the anti-CBF-A antibody followed by confocal microscopy revealed that cellular CBF-A is expressed all over in the forebrain, showing distinctive nuclear localization (Figure 3). Interestingly, a fraction of CBF-A was also found outside the cell nucleus in discrete particles, reminiscent of transported granules in oligodendrocytes, with different sizes and signal intensities depending on the brain regions analyzed (Figure 3, cf. E and M). To test whether in oligodendrocytes CBF-A displays a granular distribution, we performed triple-immunostaining of brain sections with the anti-CBF-A antibody, a rat mAb against MBP, which specifically labels myelin fibers, and a mouse mAb against 2′,3′-cyclic nucleotide 3′-phosphodiesterase (CNPase), which labels oligodendrocytes membranes and is commonly used as marker for oligodendrocytes. Remarkably, in nuclei encapsulated by CNPase we detected very little CBF-A, whereas most of the CBF-A–positive granules were found in close proximity to CNPase and/or MBP, suggesting a specialized cytoplasmic function for CBF-A, presumably in processes emanating from the cell body (Figure 3, cf. I and Q). Consistent with the in vivo distribution detected in mouse forebrain, CBF-A–positive granules were also revealed in primary oligodendrocytes, astrocytes, and neurons obtained by in vitro differentiation of fetal rat and adult mouse neural stem cells (Figure 4 and Supplementary Figure S1). In all these cases, CBF-A–positive granules were revealed along the microtubule-rich processes.

To study whether CBF-A is present in MBP mRNA granules, we used a stable mouse oligodendroglial precursor cell line, oli-neu cells, which can differentiate into myelin-associated glycoprotein (MAG)-positive oligodendrocytes (Jung *et al.*, 1995). Differentiated oli-neu cells were subjected to immunofluorescence in situ hybridization (immuno-FISH) experiments with the anti-CBF-A antibody and a specific 5′ digoxigenin end-labeled RNA probe hybridizing with the endogenous MBP mRNA RTS. Confocal microscopy revealed that CBF-A–positive granules distributed along oligodendrocytes processes partly colocalize with MBP mRNA in granular structures (Figure 5, A–H, see arrowheads in H), similar to hnRNP A2 (Figure 5, I–P, see arrows in P). In support of a colocalization between endogenous CBF-A and RTS-containing MBP mRNA, we next performed unbiased statistical analysis on the fluorescence intensity levels derived from the corresponding confocal images and as previously described (Ma *et al.*, 2002). The results revealed linear correlations between the CBF-A and RTS signals (Figure 5B). Quantification of the number of colocalization events occurring in individual particles showed that roughly 88% of the granules contains CBF-A and RTS-containing mRNA. As expected, a similar correlation was revealed between the hnRNP A2 and RTS signals (Figure 5C), where ~90% of the granules contained both hnRNP A2 and RTS-containing mRNA. Furthermore, double immunostaining experiments demonstrated a linear correlation also between the granular distributions of CBF-A and hnRNP A2 (Figure 6, A and B), and CBF-A was found to colocalize with α-tubulin along oli-neu processes (Supplementary Figure 2). Finally triple oli-neu immunofluorescence staining for the MBP mRNA RTS, hnRNP A2, and CBF-A showed that more than 80% of endogenous MBP mRNA granules were positively stained for RTS RNA, CBF-A, and hnRNP A2 (Supplementary Figure S3). We conclude that CBF-A binds RTS

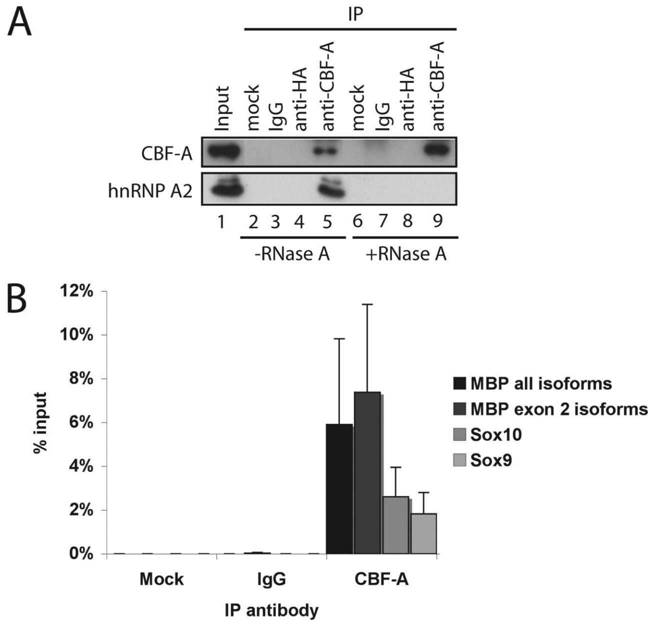

Figure 7. CBF-A is associated with MBP mRNA in differentiating oligodendrocytes. (A) A complex containing CBF-A and hnRNP A2 is coprecipitated with the anti-CBF-A antibody from total protein extracts (Input) prepared from differentiating oli-neu cells in an RNA-dependent manner. Where indicated, extracts were treated with RNase A before immunoprecipitation. Bound proteins were resolved by SDS-PAGE and analyzed on immunoblots with antibodies to CBF-A and hnRNP A2. (B) qRT-PCR was performed on reverse-transcribed cDNA derived from RNA extracts of differentiating oli-neu cells, immunoprecipitated by CBF-A. The anti-CBF-A antibody leads to enrichment of MBP mRNA, as assessed with MBP-specific primers. Mock experiments and IgG pulldowns revealed negligible RNA enrichment. Input samples were considered to be 100%; thus all samples were divided by the inputs mean value. Data are presented as average of three independent experiments. Error bars, SEM. Importantly, in each case the percentages of immunoprecipitated mRNA are relative to the total amount of each individual mRNA species (input) analyzed.

sequences and is present in MBP mRNA-containing granules.

CBF-A Is Required for Transport of MBP mRNA Granules in Oligodendrocytes

If CBF-A binds RTS sequences and accompanies MBP mRNA along oligodendrocyte processes, CBF-A may be implicated in MBP mRNA transport to the myelin compartment. To start proving this possibility, we subjected total oli-neu protein extracts treated or not treated with RNase A to immunoprecipitation experiments with the anti-CBF-A antibody. The coprecipitated fractions were monitored on immunoblots to identify some of the proteins associated with CBF-A. Consistent with our previous fractionation experiment and protein–protein interaction assays performed using HeLa cells protein extracts, the anti-CBF-A antibody specifically coprecipitated hnRNP A2 from total oli-neu cell extracts in the absence of RNase A treatment (Figure 7A, lane 5). On the contrary, hnRNP A2 was not coprecipitated with CBF-A from oli-neu extracts treated with RNase A before the immunoprecipitation experiment (Figure 7A, cf. lanes 5 and 9). Finally, CBF-A and hnRNP A2 were not coprecipitated from oli-neu cell extracts with unrelated control antibodies independently from the RNase treatment, supporting the specificity of the assay (Figure 7A, cf. lanes 3, 4 and 7, 8, respectively). These results suggest that CBF-A and hnRNP A2 are part of the same RNA-containing complexes, but they are not directly associated. To test whether CBF-A is directly associated with the MBP mRNA, total RNA was extracted from the same coprecipitated fractions using the Triazol reagent. In all cases, the percentage of precipitated RNA was analyzed by qRT-PCR using specific primers to the MBP mRNA as well as Sox10 and Sox9 mRNAs encoding nuclear transcription factors associated with terminal oligodendrocytes differentiation (Wegner and Stolt, 2005). As can be seen, the bars diagram in Figure 7 shows a significant enrichment (5.9% of the input) of exon1-containing MBP mRNA transcripts (Figure 7B), an exon that is present in all MBP isoforms (Boggs, 2006). A considerable enrichment was also observed (7.4% of the input) for the MBP mRNA isoforms that contain exon 2 (Figure 7B), an exon that is mainly expressed in the early stages of myelination (Boggs, 2006). Finally, MBP mRNA enrichment was not revealed in the control immunoprecipitated fractions (Figure 7B). We conclude that in differentiating oli-neu cells a considerable proportion of CBF-A is specifically associated with the MBP mRNA, presumably as part of MBP mRNA granules.

We next silenced the *CBF-A* gene by RNA interference (RNAi) to test for a potential direct role of CBF-A in the transport of MBP granules. Oli-neu cells were transfected with RNA duplexes against target sequences on the *CBF-A* gene. Steady-state expression of endogenous CBF-A was monitored by Western blotting on total oli-neu protein extracts and by immunofluorescence using the anti-CBF-A antibody (Figure 8, A and B), whereas the CBF-A mRNA levels were monitored by qRT-PCR (data not shown). A specific shut down of the expression resulting in a considerable decrease in endogenous CBF-A steady-state level was observed 4 d after transfection (Figure 8A). To test whether CBF-A silencing resulted in an abnormal distribution of MBP mRNA, we performed immuno-FISH on CBF-A–silenced oli-neu cells and monitored the distribution of MBP mRNA. Notably, in CBF-A–silenced oli-neu cells MBP mRNA was mainly revealed in the cell body and was not detected along processes (Figure 8B, K–T), whereas in control oli-neu cells transfected with unrelated RNAi oligonucleotides, the distribution of MBP mRNA granules along oligodendrocyte processes was not affected (Figure 8B, A–J). We conclude that CBF-A gene knockdown specifically represses MBP mRNA trafficking along oligodendrocytes processes.

In Differentiating Oligodendrocytes CFB-A Is in Cytoskeleton-associated Granules

We carried out immunoelectron microscopy to determine the distribution of CBF-A in differentiated oli-neu cells. The cells were fixed, cryosubstituted, and embedded in a resin suitable for immunoelectron microscopy. Thin sections were stained with the anti-CBF-A antibody, and the labeling was visualized using a secondary antibody conjugated to colloidal-gold markers. The abundant cellular processes characteristic of differentiated oli-neu cells were clearly visible in the preparations (Figure 9, A, C, E, and G). CBF-A was detected in different cell compartments. A significant fraction of CBF-A was located in the nucleus, as expected for an hnRNP protein (Figure 9B). We also found CBF-A associated with microtubules (Figure 9, C and D) and with microfilament bundles (Figure 9E) in the cytoplasmic processes of the oli-neu cells. Interestingly, the anti-CBF-A labeling was often observed associated with two types of dense granules

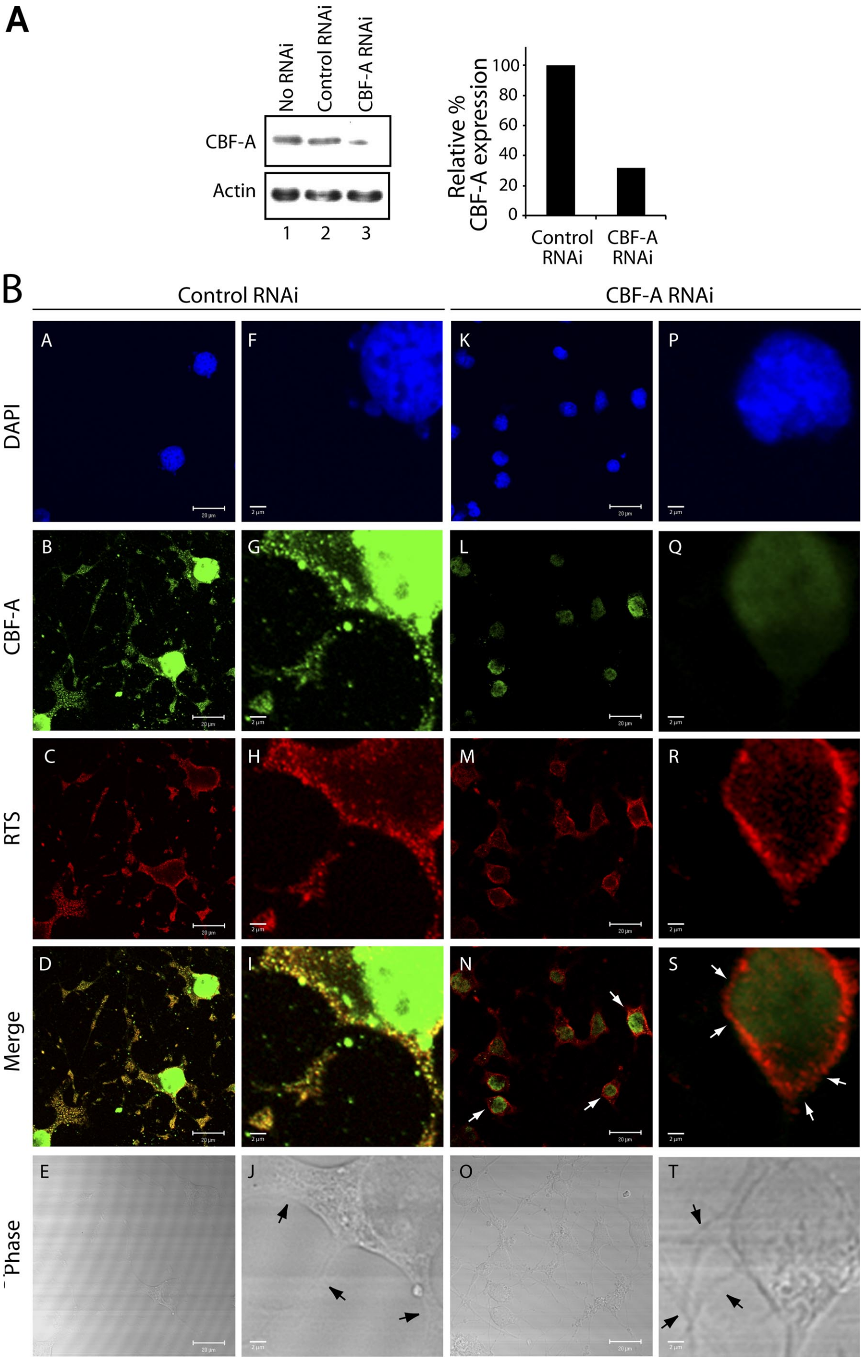

Figure 8. (A) Steady-state expression levels of CBF-A in mock-transfected oli-neu cells (lane 1), control oli-neu cells transfected with nonspecific siRNA oligonucleotides (lane 2), and in CBF-A silenced oli-neu cells (lane 3). The bars diagram shows the relative amounts of CBF-A determined in independent experiments as ratios between transfected (either with control siRNA oligonucleotides or with specific siRNA oligonucleotides against CBF-A) and mock-transfected oli-neu cells. (B) In CBF-A–silenced oli-neu cells, MBP mRNA is excluded from oligodendrocytes processes as monitored by immuno-FISH and confocal microscopy. White arrows point toward siRNA-transfected cells in which the expression of CBF-A is considerably decreased (N and S). Black arrows point toward processes of oli-neu cells that are transfected with control siRNA oligonucleotides or specific siRNA oligonucleotides to silence CBF-A (J and T). Scale bars, (A–E and K–O) 10 μm; (F–J and P–T) 10 μm. In the right column, D–T show silenced oli-neu cells at fivefold magnification. Overall, these experiments were repeated three times and on average as much as 70% of cells showed decreased expression of CBF-A and MBP mRNA exclusion from processes.

with diameters of 30–40 nm (Figure 9F) and 300–400 nm (lg in Figure 9E), respectively. These large CBF-A–positive granules correspond to the RNA transport granules observed in our immunofluorescence experiments (see *Discussion*), and their dimensions are in agreement with previous reports of MBP granules in oligodendrocytes (Ainger *et al.*, 1993; Barbarese *et al.*, 1995). Both large and small granules are found in association with the cytoskeleton. Finally, the immunoelectron microscopy experiment also revealed that CBF-A reaches the myelin compartment. Indeed, significant labeling was observed in association with the concentric multilamellar formations that are characteristic of the differentiating oligodendrocytes (Figure 9, E, G, and H).

We also analyzed the distribution of CBF-A in HeLa cells (Supplementary Figure S4). Both the nucleus and the cytoplasm were significantly labeled (Supplementary Figure S4, A and B), and gold markers were occasionally observed in the proximity of the nuclear envelope (Supplementary Figure S4C). In the cytoplasm of HeLa cells, CBF-A could also be seen in dense granules that resemble the small granules described in oli-neu cells based on dimensions, texture, and electron density. The large CFB-A granules observed in oligodendrocytes were not present in HeLa cells. Interestingly, the small CBF-A–containing granules were associated with cortical filaments and filipodia at the periphery of HeLa cells (Supplementary Figure S4, F and G).

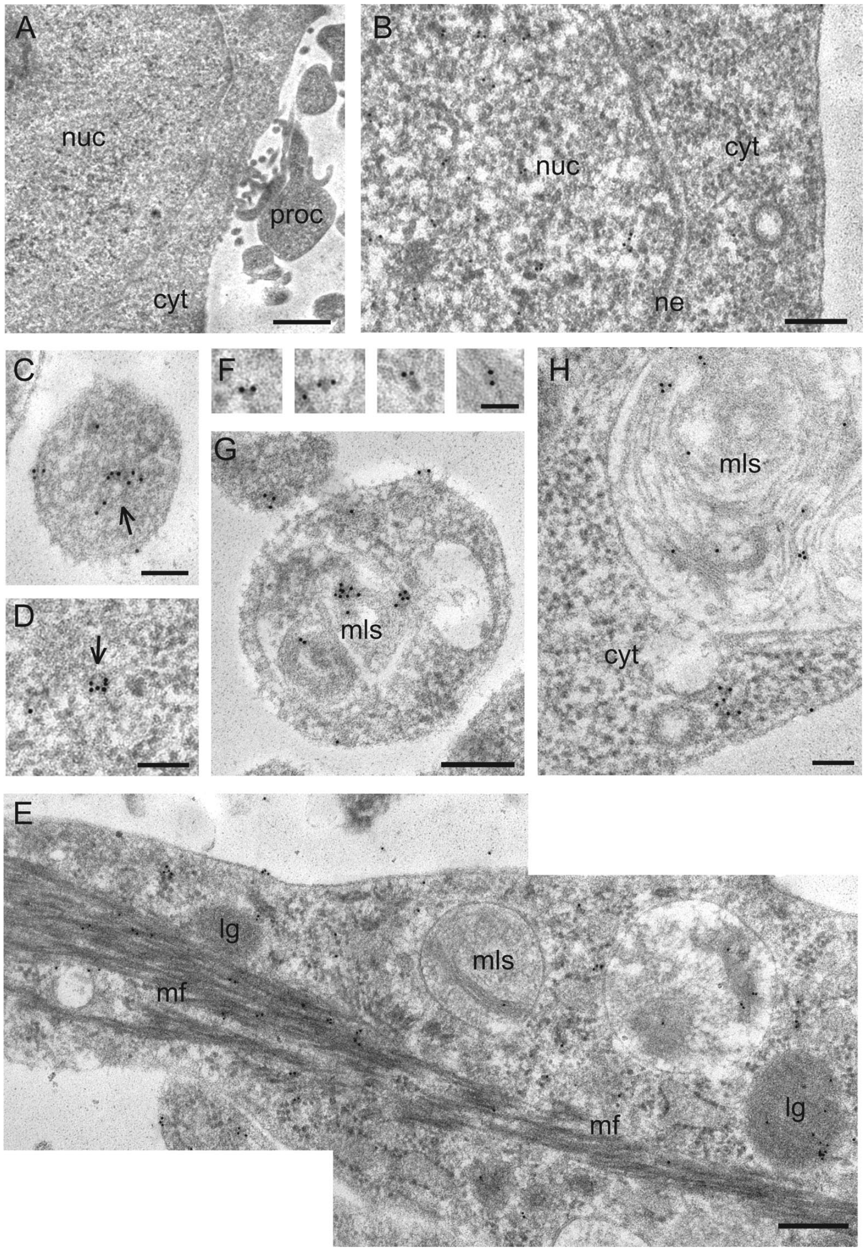

Figure 9. Immuno-EM analysis of CBF-A in oli-neu cells. (A) Overview of a typical oli-neu cell cryosubstituted and embedded in Lowicryl K4M. The nucleus (nuc), cytoplasm (cyt), and some cellular processes (proc) are indicated in the figure. (B–H) Micrographs showing the distribution of CBF-A in oli-neu cells. (B) The anti-CBF-A antibody stained both the nucleus and the cytoplasm. The nuclear envelope (ne) is clearly visible in the micrograph. (C and D) Two examples of microtubules, in transversal section, decorated by multiple gold markers (arrows). (E) Composite micrograph showing intense CBF-A labeling associated with a bundle of microfilaments (mf) in the interior of a process. Note the presence of a multilamellar structure (mls) in the process and the association of large dense granules (lg) with the cytoskeleton. (F) Four examples of cytoplasmic small granules labeled by the anti-CBF-A antibody. The small granules have a diameter of ~35 nm. (G and H) Micrographs showing typical multilamellar structures (mls) intensely decorated by gold markers. Scale bars, (A) ~1 μm; (B, C and E) 200 nm; and (D, F, G, and H) 100 nm.

DISCUSSION

In summary, we provide evidence that CBF-A is a novel transacting factor required for MBP mRNA transport and localization. Consistent with this view, RNA pulldown experiments and EMSA demonstrated direct binding of CBF-A to the MBP RTS, and immuno-FISH showed a correlation between the CBF-A distribution and MBP mRNA granules. CBF-A posttranscriptional gene silencing resulted in MBP mRNA retention in the oligodendrocytes cell body. Furthermore, the in vivo distribution of CBF-A in adult mouse forebrain indicates that CBF-A–positive granules are preferentially found in those areas of the mouse forebrain where myelin fibers appear to be loose or decompacted. Finally, the immunoelectron microscopy experiments showed that in the cytoplasm of differentiating oli-neu cells CBF-A is found in dense granules, is associated with microfilaments and microtubules in the processes and is transported to multilamellar structures that resemble the membrane formations observed in the myelin compartment of oligodendrocytes in vivo. In view of our results, we propose that in oligodendrocytes, CBF-A plays a specialized and key role in MBP biogenesis mediating MBP mRNA transport to the peripheral myelin compartment for constitutive MBP production.

CBF-A and hnRNP A2 are both present in MBP mRNA granules, and they are both required for MBP mRNA transport and localization. These observations raise the question as to why the same mRNA granule requires the presence of at least two transacting factors. At this stage it is rather difficult to address this issue at the molecular level. However, the linear correlations on the fluorescence signals observed between CBF-A and MBP mRNA, between hnRNP A2 and MBP mRNA as well as between CBF-A and hnRNP A2, and the fact that CBF-A and hnRNP A2 can be coimmunoprecipitated in an RNA-dependent manner overall suggest that CBF-A and hnRNP A2 are simultaneously present in the same MBP mRNP complex. If this is the case, CBF-A and hnRNP A2 may cooperate for MBP mRNA transport and localization. Their roles could be dependent on the local environment and the set of interactions required for the establishment of trafficking intermediates, for instance, to determine polarity during RNA trafficking (Carson and Barbarese, 2005).

CBF-A is ubiquitously expressed and has been suggested to have a role in transcriptional control (Kamada and Miwa, 1992; Bemark *et al.*, 1998; Leverrier *et al.*, 2000; Mikheev *et al.*, 2000). Because it is also a component of shuttling pre-mRNP/mRNP particles (Percipalle *et al.*, 2002), our results suggest that CBF-A associates with mRNAs in the cell nucleus and accompanies its target mRNAs to their cytoplasmic destination. In support of this hypothesis the immunoelectron microscopy performed with our anti-CBF-A antibody in oli-neu and HeLa cells showed that CBF-A localizes in the nucleoplasm (Figure 9B and Supplementary Figure S4B). Occasionally, CBF-A was found at or near nuclear pores (Supplementary Figure S4C), which is consistent with the proposal that CBF-A remains associated with the mRNP during nucleo-cytoplasmic transport. In the cytoplasm of oli-neu and HeLa cells, CBF-A was often found in dense granules with a diameter of 30–40 nm (Figure 9F and Supplementary Figure S4, D and E). These CBF-A–containing granules, which were often seen in association with cytoskeletal fibers, are likely to be mRNA transport granules. In either case, our observations underscore the general idea that the cytoplasmic fate of each mRNA is predetermined by the assembly of the mRNP complex in the cell nucleus (Daneholt, 2001).

We revealed CBF-A–positive granules in astrocytes and neurons where mRNA transcripts containing RTS-like sequences were identified by computational approaches (Ainger *et al.*, 1997). Moreover, CBF-A was found associated with the cytoskeleton in HeLa cells. Altogether these observations, strongly suggest that CBF-A has a role in cytoplasmic mRNA transport and its function may not be exclusive of oligodendrocytes.

Given the ubiquitous distribution of CBF-A and its specific role in MBP mRNA transport in oligodendrocytes, we suggest that CBF-A has a general role as a transacting factor in the establishment of asymmetric mRNA and/or protein distributions. CBF-A is likely to act on the localization of multiple mRNAs in HeLa cells as well as in other cell types, the MBP mRNA being a specific case related to a very specialized cellular function.

ACKNOWLEDGMENTS

We thank Sonia Ruíz and Gema Martínez (Serveis Cientificotècnics, Universitat de Barcelona) for EM sample preparation. This work was supported by grants from the Swedish Research Council (Vetenskapsrådet) to P.P. and N.V. G.C.B. is supported by postdoctoral fellowships from the Swedish Brain Foundation (Hjärnfonden) and from the David and Astrid Hageléns Foundation.

REFERENCES

Ainger, K., Avossa, D., Morgan, F., Hill, S. J., Barry, C., Barbarese, E., and Carson, J. H. (1993). Transport and localization of exogenous myelin basic protein mRNA microinjected into oligodendrocytes. J. Cell Biol. *123*, 431–441.

Ainger, K., Avossa, D., Diana, A. S., Barry, C., Barbarese, E., and Carson, J. H. (1997). Transport and localization elements in myelin basic protein mRNA. J. Cell Biol. *138*, 1077–1087.

Barbarese, E., Koppel, D. E., Deutscher, M. P., Smith, C. L., Ainger, K., Morgan, F., and Carson, J. H. (1995). Protein translation components are colocalized in granules in oligodendrocytes. J. Cell Sci. *108*, 2781–2790.

Boggs, J. M. (2006). Myelin basic protein: a multifunctional protein. Cell Mol. Life Sci. *63*, 1945–1961.

Bemark, M., Olsson, H., Heinegård, D., and Leanderson, T. (1998). Purification and characterization of a protein binding to the SP6 k promoter. J. Biol. Chem. *273*, 18881–18890.

Carson, J. H., Cui, H., Krueger, W., Schlepchenko, B., Brumwell, C., and Barbarese, E. (2001). RNA trafficking in oligodendrocytes. Results Probl. Cell Differ. *34*, 69–81.

Carson, J. H., and Barbarese, E. (2005). Systems analysis of RNA trafficking in neural cells. Biol. Cell *97*, 51–62.

Daneholt, B. (2001). Assembly and transport of a pre-messenger RNP particle. Proc. Natl. Acad. Sci. USA *98*, 7012–7017.

Dean, J.L.E., Sully, G., Wait, R., Rawlinson, L., Clark, A. R., and Saklatvala, J. (2002). Identification of a novel AU-rich-element-binding protein which is related to AUF1. Biochem. J. *366*, 709–719.

Deshler, J. O., Highett, M. I., and Scnapp, B. J. (1997). Localization of *Xenopus* Vg1 mRNA by Vera protein and the endoplasmic reticulum. Science *276*, 1128–1131.

Dreyfuss, G., Matunis, M. J., Pinõl-Roma, S., and Burd, C. G. (1993). hnRNP proteins and the biogenesis of mRNA. Annu. Rev. Biochem. *62*, 289–321.

Dreyfuss, G., Kim, V. N., and Kataoka, N. (2002). Messenger-RNA-binding proteins and the messenger they carry. Nat. Rev. Mol. Cell Biol. *3*, 195–205.

Elvira, G. *et al.* (2006). Characterization of an RNA granule from developing brain. Mol. Cell Proteomics *5*, 635–651.

Gielen, E., Baron, W., Vandeven, M., Steels, P., Hoekstra, D., and Ameloot, M. (2004). Rafts in oligodendrocytes: evidence and structure-function relationship. Glia *54*, 499–512.

Hoek, K. S., Kidd, G. J., Carson, J. H., and Smith, R. (1998). hnRNP A2 selectively binds the cytoplasmic transport sequence of myelin basic protein mRNA. Biochemistry *37*, 7021–7029.

Hüttelmaier, S., Zenklusen, D., Lederer, M., Dictenberg, J., Lorenz, M., Meng, X., Bassell, G. J., Condeelis, J., and Singer, R. H. (2005). Spatial regulation of beta-actin translation by Src-dependent phosphorylation of ZBP1. Nature *438*, 432–435.

Jung, M. *et al.* (1995). Lines of murine oligodendroglial precursor cells immortalized by an activated neu tyrosine kinase show distinct degrees of interaction with axons in vitro and in vivo. Eur. J. Neurosci. *7*, 1245–1265.

Kamada, S., and Miwa, T. (1992). A protein binding to CArG box motifs and to single-stranded DNA functions as transcriptional repressor. Gene *119*, 229–236.

Kanai, Y., Dohmae, N., and Hirokawa, N. (2004). Kinesin transports RNA: isolation and characterization of an RNA-transporting granule. Neuron *43*, 513–525.

Kiledjian, M., and Dreyfuss, G. (1992). Primary structure and binding activity of the hnRNP U protein: binding RNA through RGG box. EMBO J. *11*, 2655–2664.

Krecic, A. M., and Swanson, M. S. (1999). hnRNP complexes: composition, structure and function. Curr. Opin. Cell Biol. *11*, 363–371.

Leverrier, S., Cinato, E., Paul, C., Derancourt, J., Bemark, M., Leandersson, T., and Legraverend, C. (2000). Purification and cloning of type A/B hnRNP proteins involved in transcriptional activation from the rat spi2 gene GAGA box. Biol. Chem. *381*, 1031–1040.

Ma, A.S.W., Moran-Jones, K., Shan, J., Munro, T. P., Snee, M. J., Hoek, K. S., and Smith, R. (2002). Heterogeneous nuclear ribonucleoprotein A3, a novel RNA trafficking response element-binding protein. J. Biol. Chem. *277*, 18010–18020.

Mikheev, A. M., Mikheev, S. A., Zhang, Y., Aebersold, R., and Zarbl, H. (2000). CArG binding factor A (CBF-A) is involved in transcriptional regulation of the rat Ha-ras promoter. Nucleic Acids Res. *28*, 3762–3770.

Palacios, I., and St. Johnson, D. (2001). Getting the message across: the intracellular localization of mRNAs in higher eukaryotes. Annu. Rev. Cell Dev. Biol. *17*, 569–614.

Percipalle, P., Jonsson, A., Nashchekin, D., Karlsson, C., Bergman, T., Guialis, A., and Daneholt, B. (2002). Nuclear actin is associated with a specific subset of hnRNP A/B-type proteins. Nucleic Acids Res. *30*, 1725–1734.

Percipalle, P., and Visa, N. (2006). Molecular functions of nuclear actin. J. Cell Biol. *172*, 967–971.

Rietze, R. L., and Reynolds, B. A. (2006). Neural stem cell isolation and characterization. Methods Enzymol. *419*, 3–23.

Ross, A., Oleynikov, Y., Kislauskis, E., Taneja, K., and Singer, R. (1997). Characterization of a beta actin mRNA zipcode-binding protein. Mol. Cell. Biol. *17*, 2158–2165.

Shav-Tal, Y., and Singer, R. H. (2005). RNA localization. J. Cell Sci. *118*, 4077–4081.

Sidman, R. L., Kosaras, B., Misra, B., and Senft, S. (2008). High resolution mouse brain atlas. Harvard University Brain Atlas Project. http://www.hms.harvard.edu/research/brain/atlas.html/. (accessed 5/9/08).

Singer, R. H., and Ward, D. C. (1982). Actin gene expression visualized in chicken muscle tissue culture by using in situ hybridization with a biotinylated nucleotide analog. Proc. Natl. Acad. Sci. USA *79*, 7331–7335.

Smith, R. (2004). Moving molecules: mRNA trafficking in Mammalian oligodendrocytes and neurons. Neuroscientist *10*, 495–500.

Wegner, M., and Stolt, C. C. (2005). From stem cells to neurons and glia: a Soxist's view of neural development. Trends Neurosci. *28*, 583–588.